

Towards a crystal undulator

S H Connell¹, J Hartwig², A Masvaure¹, D Mavunda^{1,3} and T N Tran Thi¹

¹ University of Johannesburg, Johannesburg, South Africa

² European Synchrotron Radiation Facility (ESRF), Grenoble, France

³ Nuclear Energy Corporation of South Africa (Necsa), South Africa

E-mail: shconnell@uj.ac.za

Abstract. The CUTE FP7 project proposes to produce ultimately a MeV range gamma ray laser by the FEL principal in a crystal undulator. The GeV range electron beam would need to be captured in a low index crystallographic channel of a crystal superlattice, in such a way that the varying electrostatic crystalline field would resemble a Tesla range periodically varying magnetic field with a few micron pitch, when viewed in the reference frame of the undulating electron or positron. We have investigated a prototype diamond superlattice using x-ray diffraction topography. The undulator fabrication principle involved CVD growth of diamond on a diamond substrate while varying the concentration of boron in the gas phase during growth. This should lead to the periodic variation of the lattice dilatation by the varying concentration of the single substitutional boron impurity atom. The validation via x-ray diffraction topography proved non-trivial but was eventually promising.

1. Introduction

A crystal undulator is similar to a normal undulator as typically found at a synchrotron for the production of extremely brilliant X-ray beams. The difference is the magnetic lattice is realized by the periodic electrostatic potential of a crystal lattice seen from the reference frame of the GeV range electron or positron beam. The extremely relativistic incident particle beam would need to be captured in a high index crystallographic channel of a crystal superlattice. The particle beam will then see a many Tesla range periodically varying magnetic field with a micron scale pitch. This method could theoretically lead to an MeV range gamma ray laser by the FEL principal.

We have investigated a prototype diamond superlattice using x-ray diffraction topography at the ESRF. The undulator fabrication principle involved CVD growth of boron doped diamond on a diamond substrate while varying the concentration of boron in the gas phase during growth. This should lead to the periodic variation of the lattice dilatation corresponding to the varying concentration of the single substitutional boron impurity atom. This is the realisation of the diamond superlattice, which has periodic layers of graded composition, coherently registered on each other, with a smoothly varying periodic lattice constant.

2. Parameters for the crystal undulator and its realisation

The theoretical feasibility study to produce powerful monochromatic undulator radiation in the gamma ray region by means of a crystal undulator (periodically bent crystal) and

ultra relativistic light lepton beams impinging on the lattice with aligned incidence to a crystallographic axis is presented in several references [1, 2, 3] and references therein.

Figure 1 indicates the trajectory of a charged particle captured in the channeling condition in a low index crystallographic direction. The channelled trajectory has an oscillation within the channel, leading to the emission of lower energy channeling radiation. In addition the particle follows the periodic undulations of the lattice, and as such, it will also emit MeV range undulator radiation.

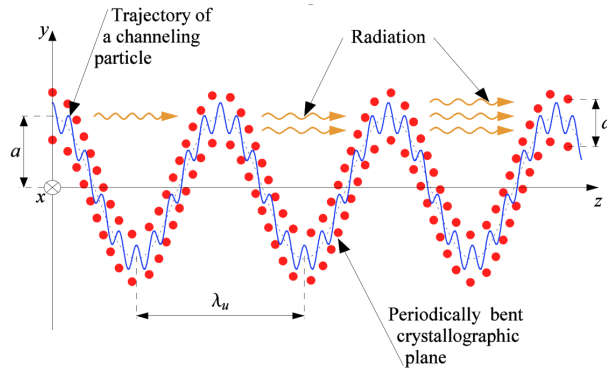


Figure 1. A charged particle captured in a undulating crystal channel, indicated by the periodically bent lattice of dots.

The parameters of the crystal undulator are typically in the range shown in table 1, where an important condition is $\lambda_u \gg a \gg d$.

Table 1. Typical physical parameters for a crystal undulator.

Undulator wavelength = λ_u	≈ 0.1 mm
Undulator amplitude = a	≈ 50 Å
Interplanar distance = d	1 – 2 Å
Crystal thickness = t	1 – 4 mm
Number of oscillations = $N_u = t/\lambda_u$	10

These parameters are obtained considering the energy and particle type dependent dechanneling length and the beam and crystal physical properties. Diamond suggests itself as a premier material for a crystal undulator for several reasons. The lattice is extremely radiation hard (it sustains 1×10^{15} mips/cm²). This consideration is of special importance for a material that could conceivably withstand the beam bunch intensities for the SASE (Self Amplified Spontaneous Emission) version of the crystalline undulator. The high Debye temperature results in diminished latticed vibrations, which increases the dechanneling length. This also enhances the coherence length for phenomena which are associated with radiation emission. The low atomic number leads to a lower channelling potential but this is offset somewhat by the very high atomic packing density. The $\langle 110 \rangle$ channelling direction in diamond is particularly favourable for the channelling of positive particles, as both the core spatial distribution and the electron spatial distribution contribute to a deep potential well which is well separated from sources of hard scattering.

Previous attempts to fabricate a diamond crystal undulator deployed the permanent periodic deformation of the diamond by inducing a periodic surface strain using a laser scoring procedure

[4]. As the surface strain relaxes towards the bulk, this method produced a distribution of undulator amplitudes. The monochromaticity of the energy of the undulator radiation depends on all transmitted channeled particles experiencing the same undulator amplitude, and so the surface deformation technique is not suitable [5].

This has led to the need for the development of a graded superlattice, as an alternative method to produce a crystal undulator.

3. The diamond graded superlattice

Doping diamond with single substitutional atoms of either nitrogen or boron dilates the lattice. Both of these atoms are soluble in diamond, and can be introduced during the growth of synthetic diamond in the CVD process in a regulated way. It is in fact the case that one must go to considerable lengths to exclude these dopants should one desire intrinsic diamond (considered as having impurity concentrations in the low ppb range). The lattice dilatation for nitrogen [6] (single substitutional) is

$$\frac{\Delta a}{a_0} = 0.125 \pm 0.006 \times C_N,$$

while that for boron [7, 8, 9] (single substitutional) is

$$\frac{\Delta a}{a_0} = 0.144 \times C_B.$$

C_N and C_B are the atomic concentrations of nitrogen and boron respectively as fractions. For the purpose of deliberate lattice dilation under conditions of minimising extended defects and more complex point defects (dislocations, stacking faults, interface coherence, aggregation) boron is favoured. Experience has shown that one may obtain even heavily doped boron concentrations of $C_B < 1.5$ at% while still maintaining excellent local lattice quality. In exceptional cases, the interface definition can be on the nanometric, near atomic, scale [10].

The undulator amplitude to be achieved by a dilatation at each lattice site over the undulator period (see table 1) requires

$$n\Delta a = \left(\frac{d}{a_0}\right) \Delta a = 50\text{\AA}.$$

Using the dilatation formula for boron incorporation (above) and considering a 45° channeling trajectory with respect to layers of the superlattice, we find a maximum doping level of $C_B = 1000$ ppm is required. Accordingly, Element Six Technologies prepared the samples as indicated in figure 2 below, as a pilot study of the graded diamond super lattice principle. The substrates for epitaxial CVD overgrowth are High Pressure High Temperature (HPHT) synthetic diamond type Ib. It is well known that the substrate lattice quality affects the lattice quality of the CVD layer [11]. In this case no special attention was made to select high quality substrates, as this was a first proof of principle investigation. This could be seen in this study as the typical clusters of dislocations threading through the CVD layer, originating at imperfections in the substrate. A future study would select for substrates which were clear of extended defects, as was done in the reference [11].

4. Characterisation with X-ray diffraction techniques

The graded boron doped layer was studied with various X-ray diffraction techniques at the ESRF in Grenoble, beam line BM05. The X-ray photon energy was 20 keV and the reflection studied was the (400) reflection with a Bragg angle of $\theta_B = 14.23^\circ$. This study was rather difficult, as the thickness of the layer falls between two techniques for investigation of this type of local lattice parameter changes. On the smaller scale, there are interferometric techniques, and on

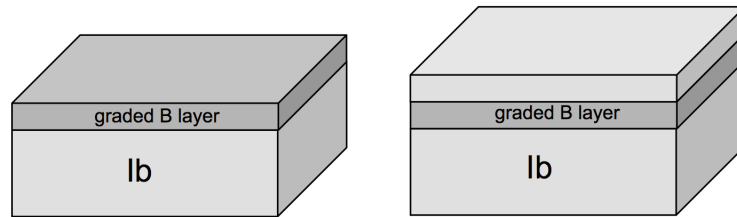


Figure 2. 50 μm thick graded B-doped layer (CVD) on a Ib diamond substrate (side 4 mm). The layer profile is triangular, extending to 3000 ppm. The sample on the right is capped with an additional "intrinsic" layer of diamond ($C_B < 50$ ppm).

the larger scale there are differential sectioning techniques. Considerable effort has therefore been expended to study these graded B-doped layers.

We report here on the investigations using plane wave monochromatic diffraction. This means the incident beam was highly collimated and monochromatic, essentially with an effective energy width which is larger but comparable to the acceptance of the actual sample crystal and reflection used. The theoretical reflectivity curve of the Si-(111) monochromator is about 4° and that for the C^* -(400) diamond sample is about 0.75° . Furthermore, the configuration was in the dispersive mode, which arises because the monochromating crystal and reflection were different to that of the sample crystal and reflection, and neither crystal was bent. This means that the Bragg condition is typically satisfied for only a given spatial range of the sample crystal, where this spatial range is a narrow band perpendicular to the incident direction of the beam. The image selected in figure 3 below is an integral of an angular rocking curve scan, so that a full rocking curve is integrated for each pixel on the sample surface.

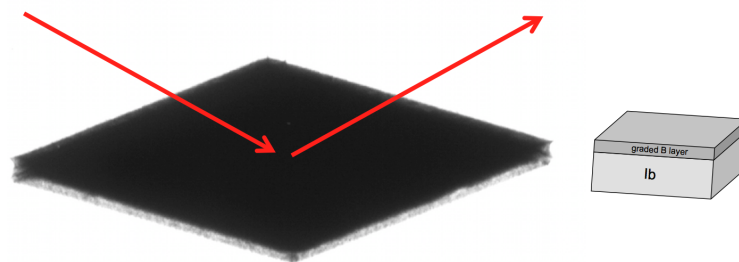


Figure 3. An integral of a rocking curve scan for the (400) reflection in the Bragg case in plane wave monochromatic diffraction.

The diffraction vector is parallel to the maximal change of the lattice constant in the graded doped layer. The geometry chosen presents a perspective view of the diamond crystal. The penetration depth of the x-ray beam is a complex mix of effects related to the angular and energy dispersion of the beam, the quality of the crystal, and the angle at which the rocking curve is taken. As discussed, in this case, the image presented is the integral of the full rocking curves for each pixel of the sample surface. The reflectivity of the graded doped layer appears significant over the whole crystal surface. It is interesting to first evaluate that the graded layer has a spread of lattice parameters (due to the range of dilatation) that corresponds to a spread of effective local diffracting angles, $\Delta d/d \approx 10^{-4}$ corresponding to $\Delta\theta \approx 21 \gg \theta_D$, the theoretical reflectivity curve for diamond, the Darwin width. This is the condition for multi-layer mirror

behaviour. There is a continuous variation of the lattice constant over a relatively shallow depth in such a way that the acceptance of the crystal in the graded doped layer is much wider than the reflectivity curve of the interrogating beam. This means that the graded doped layer can yield an integral reflectivity which is much larger than the substrate of higher lattice quality diamond. As we can see in the perspective view, where the edge is not screened by the surface layer, one can separate the graded layer and the substrate. Within the substrate, one still has the usual view of the defects within. This is because the defects once again create a local strain which also broadens the local reflectivity curve. What is important here is that we see clear evidence for successful implementation of the graded B-doped layer.

In the next figure 4, a plane wave monochromatic dispersive case topograph at just a single point on the flank of the rocking curve is presented. The geometry used optimises the view of the sample edge. It was taken with a shield over the diamond main surface to reduce the Laue case component of the diffraction and emphasise the more surface sensitive Bragg case diffraction. A component of the strain due to the dilatation should still be visible, and this seems to be the case. The analysis of the image shows a variation of the local Bragg angle across the edge where the graded B-doped layer is visible.

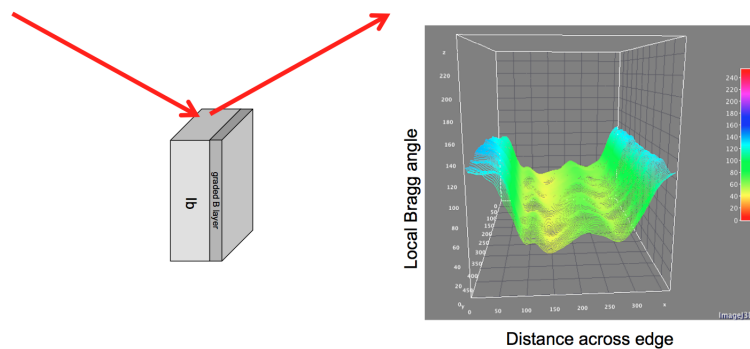


Figure 4. A plane wave monochromatic dispersive case topograph at just a single point on the flank of the rocking curve is presented with a view of the sample edge.

5. Conclusion

This paper has reported on a pilot study to produce and characterise graded B-doped superlayers. This has proved to be a non-trivial task due to the length scale of the layers. The pitch of the layer is much larger than the nano-scale, so the interference effects from Bragg scattering normal to the layer are not visible. The pitch of the layer is nonetheless somewhat small to use collimation in the entrance and exit channel to section the diffracting volume within the crystal. A large data set of both Bragg and Laue condition Rocking Curve Imaging measurements and Plane Wave Topography measurements indicated that indeed the lattice parameter variation for the superlattice could be detected. Two examples have been presented in this paper. Indeed, the lattice parameter evolves over the depth of the graded layer. The graded B-doped layer acts as an effective multi-layer mirror. The studies are continuing. It would be preferable to develop the graded layer on the best possible (lattice) quality substrates. This is the start of the iterative process to produce a diamond crystal undulator, for the first time, and the results are promising.

References

- [1] Tabrizi M, Korol A V, Solovyov A V and Greiner W 2007 *Physical Review Letters* **98** 164801
- [2] Korol A V, Solovyov A V and Greiner W 1998 *Journal of Physics G* **24** L45

- [3] Korol A V, Solovyov A V and Greiner W 1999 *International Journal of Modern Physics* **E8** 49
- [4] Balling P, Esberg J, Kirsebom K, Le D Q S, Uggerhoj U I, Connell S, Haertwig J, Masiello F and Rommeveaux A 2009 *Nuclear Instruments and Methods in Physics Research B* **267** 29522957
- [5] Kostyuk A, Korol A, Solovyov A and Greiner W 2009 *Nuclear Instruments and Methods in Physics Research B* **266** 972987
- [6] Bragg W and Bragg W 1913 *Proceedings of the Royal Society (London)* **89A** 277–290
- [7] Brunet F, Germi P, Pernet M, Deneuve A, Gheeraert E, Laugier F, Burdin M and Rolland G 1998 *Diamond and Related Materials* **7** 869–873
- [8] Brazhkin V V, Ekimov E A, Lyapin A G, Popova S V, Rakhmanina A V, Stishov S M, Lebedev V M, Katayama Y and Kato K 2006 *Physical Review B* **74** 140502
- [9] Wojewoda T, Achatz P, Ortéga L, Omnés F, Marcenat C, Bourgeois E, Blase X, Jomard F and Bustarret E 2008 *Diamond and Related Materials* **17** 1302–1306
- [10] El-Hajj H, Denisenko A, Bergmaier A, Dollinger G, Kubovic M and Kohn E 2008 *Diamond and Related Materials* **17** 409–414
- [11] Martineau P M, Gaukroger M P, Guy K B, Lawson S C, Twitchen D J, Friel I, Hansen J O, Summerton G C, Addison T P G and Burns R 2009 *Journal of Physics: Condens. Matter* **21** 364205